Transcranial Magnetic Stimulation for Modeling Alzheimer's Disease: A Neural Dynamics Approach with Pre-training

Guowei Huang[1] , Yin Tian[1,2,*]

1. School of Life and Health Information Science and Engineering, Chongqing University of Posts and Telecommunications, Chongqing, 400065, China

2. School of Computer Science and Technology, Chongqing University of Posts and Telecommunications, Chongqing, 400065, China

* Corresponding author: tianyin@cqupt.edu.cn

Abstract

Alzheimer's disease (AD) is a neurodegenerative disorder with limited treatment options. While transcranial magnetic stimulation (TMS) has demonstrated therapeutic potential, its underlying mechanisms and personalized applications are not yet fully explored. This study integrates deep learning with neurodynamics, employing a pretrained resting-state AD self-supervised model to constrain dynamic training and simulate TMS-induced neural dynamics in AD patients. The results reveal regional heterogeneity, showing enhanced excitability in stimulated regions, in contrast to reduced global neural dynamics. We identified significant differences in brain responses between AD patients and healthy controls, which provide critical theoretical support for developing TMS treatment strategies. These insights advance the understanding of AD pathophysiology and highlight the potential of TMS interventions, which may lead to more effective therapeutic approaches.

Keywords: Alzheimer's disease; neurodynamics; MAE; pre-training model

Introduction

Alzheimer's disease (AD), the most prevalent neurodegenerative disorder (Self & Holtzman, 2023), is characterized by progressive neuronal degeneration in the cerebral cortex and hippocampus, leading to cognitive decline and various non-cognitive symptoms. Current clinical management of AD primarily relies on pharmacological interventions, including cholinesterase inhibitors and NMDA receptor antagonists. However, these therapeutic approaches have demonstrated limited efficacy in halting disease progression (Marucci et al., 2021). Given these limitations, there is an increasing focus on exploring novel non-pharmacological strategies to ameliorate clinical symptoms and potentially decelerate disease progression in AD patients.

Among emerging non-invasive interventions, transcranial magnetic stimulation (TMS) has garnered significant attention in the field of neurodegenerative disease treatment. Research indicates that TMS can effectively modulate cortical neural activity, demonstrating substantial improvements in cognitive functions and emotional states, particularly in AD interventions (Koch et al., 2022). The therapeutic mechanisms of TMS primarily involve the enhancement of cortical synaptic plasticity and the improvement of inter-regional brain connectivity, thereby offering potential benefits in addressing cognitive dysfunction and emotional disturbances in AD patients. Despite promising clinical trial outcomes, several critical issues remain unresolved, including the need for long-term efficacy data, optimization of personalized treatment parameters, and comprehensive safety evaluations.

For instance, Xiu et al. (2024) conducted a systematic evaluation of high-frequency repetitive transcranial magnetic stimulation (rTMS) in treating cognitive and emotional disorders in AD patients. Their findings revealed that while high-frequency rTMS significantly improved cognitive functions in certain AD patients, substantial inter-individual variability in treatment response was observed. These results underscore the necessity for further research to elucidate TMS's potential therapeutic value in AD treatment and to address the challenges posed by individual response variability.

In parallel with these developments, innovative computational approaches are being explored. The Masked Autoencoder (MAE), an advanced self-supervised learning framework, has demonstrated remarkable capabilities in reconstructing complete data distributions through random input masking and deep feature extraction (He et al., 2022). This methodology has shown particular promise in image processing and computer vision applications, and is increasingly being adapted for neurological data analysis to uncover latent patterns and enhance diagnostic and therapeutic strategies.

Building upon these advancements, pre-training and fine-tuning strategies, which form the cornerstone of modern deep learning approaches, have been extensively applied across various domains including natural language processing (NLP) and computer vision (CV) (Brown et al., 2020; Chen et al., 2023). These strategies typically employ a cascaded training paradigm, where models first acquire general feature representations through large-scale dataset pre-training, followed by task-specific fine-tuning. In the context of electroencephalogram (EEG) signal processing for AD diagnosis, this approach can be effectively implemented by first pre-training models on resting-state EEG data from both AD patients and healthy controls (HC), followed by fine-tuning on larger AD-specific EEG datasets to enhance model performance in reconstructing AD-related neural patterns.

These neural activity patterns can be effectively captured through non-invasive neuroimaging techniques, reflecting the functional state of the nervous system (Bricault et al.,

In D. Barner, N.R. Bramley, A. Ruggeri and C.M. Walker (Eds.), *Proceedings of the 47th Annual Conference of the Cognitive Science Society*

2024; Griffiths et al., 2021). Whole-brain modeling (WBM) conceptualizes the brain as a complex network of interconnected functional regions (Elam et al., 2021), where each node represents a neuronal population in a specific brain area, generating observable signals through electrophysiological activity. The connection weights between nodes are determined based on neuroimaging or anatomical data, with dynamic models simulating potential changes that are integrated into a comprehensive whole-brain network through connection matrices. This modeling approach not only simulates the propagation of local neuronal activity across the brain but also replicates whole-brain response patterns to external stimuli.

Building upon these advancements, this study introduces an innovative AD neural dynamics modeling framework DynAD-net. This framework employs masked autoencoders (MAEs) to construct a pre-trained model of AD resting states and establishes a dynamic neural model through fine-tuning strategies, enabling accurate simulation of TMS effects on the cerebral cortex, particularly in the M1 region associated with cognitive function. The framework effectively reduces the characteristic distance between stimulation intervals and AD resting states by implementing resting state connection constraints, thereby generating TMS stimulation interval functional connections that more accurately reflect real AD neural dynamics. During the evaluation phase, the framework successfully simulates personalized AD-TMS response data through the incorporation of individualized AD functional connectivity matrices.

The primary contributions of this study can be summarized as follows:

1.This study presents DynAD-net, a pre-trained model optimizing resting-state data and error constraints to improve AD analysis. It addresses traditional limitations and advances disease mechanism exploration.

2.We adopted a whole-brain transfer modeling approach, trained on normal subjects and applied to AD patients. It tackles data scarcity and enables cross-population research and precision interventions.

3.We implemented personalized TMS response simulation and dynamic feature analysis. This innovation enhances TMS understanding and facilitates individualized therapy design.

The structure of this paper is organized as follows: Section 2 provides a comprehensive review of relevant research; Section 3 details the implementation methodologies for pretraining and fine-tuning models, along with dynamic model constraint strategies; Section 4 presents experimental results and analyses; and the final section summarizes research findings and outlines future research directions.

Related Works

Whole-brain modeling integrates multimodal neuroimaging data (e.g., DTI, fMRI) with computational models to bridge neuroimaging and brain function mechanisms (Lavanga et al., 2023; Mindlin et al., 2024). Using differential equations and anatomical networks, these models simulate brain activity, enabling hypothesis testing and investigation of counterfactual scenarios like structural lesions or functional perturbations. This approach is valuable for understanding brain disorders and developing therapies.

Whole-brain models fall into two categories: (1) simplified models focusing on universal neural dynamics, ideal for exploring general network properties (López-González et al., 2021); and (2) complex models incorporating detailed biophysical mechanisms, such as neurotransmitter distributions and transcriptomic data, offering higher biological fidelity (Sanchez-Rodriguez et al., 2018; Burt et al., 2021). These complementary approaches balance computational efficiency and accuracy for diverse neuroscience research.

Methods

This section outlines the DynAD-net framework, including neural dynamics modeling, pretraining, and constraints. MAE pretrains on AD resting-state data to extract key features. Figure 1 illustrates the entire architecture of our framework. Neural dynamics optimization minimizes differences between TMS intervals and AD resting states, enabling precise AD dynamics simulation. In the evaluation phase, individualized AD connectivity matrices are used to simulate whole-brain TMS responses, comparing AD patients and healthy controls. This reveals TMS-induced brain activity differences and supports personalized AD-TMS therapy development.

Dynamics Module

This study constructs structural connectivity matrices from DWI data using fiber bundle counts. The Parcel Schaefer atlas divides the brain into 200 functional regions The Parcel Schaefer atlas divides the brain into 200 functional regions (Burt et al., 2021) , covering major cortical networks. Each region is represented by an equivalent dipole, with neuronal activity simulated by a neural dynamics model that captures TMS-induced depolarization and perturbation effects.By integrating neuronal activity with fiber connectivity, we built a network model simulating whole-brain TMS perturbations.The Neural Mass Model (NMM) simulates postsynaptic potential dynamics across 200 regions, while EEG source imaging maps these potentials to the scalp (Kaur et al., 2022), enabling cross-scale simulation from neuronal activity to EEG signals. This approach precisely models TMS-induced EEG responses and supports TMS neuromodulation optimization.

To enhance biological plausibility and clinical relevance, we integrated a self-supervised MAE model, trained on AD resting-state data, into the DynAD-net framework. AD resting-state features constrain model optimization, ensuring functional connectivity patterns reflect AD characteristics. This enables precise simulation of personalized TMS strategies and advances AD neuromodulation research.

The Jansen-Rit model, a core component, uses coarse-grained modeling to simulate three neuronal populations: pyramidal cells, inhibitory interneurons, and excitatory interneurons. Three coupled differential equations describe their interactions and responses to TMS.

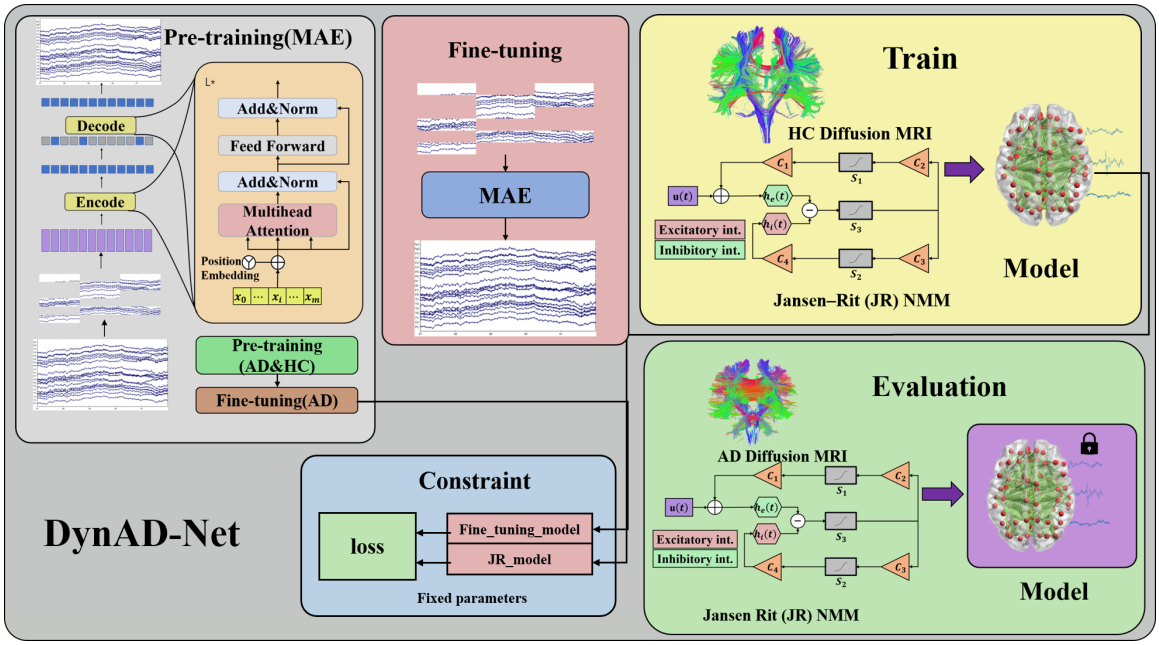

Figure 1: DynAD-Net framework, including pre-training module, fine-tuning model, dynamics training module, constraint module and AD migration mode.

1.Excitatory neurons

$$\dot{v}_{j1} = x_{j1} \tag{1}$$

$$\dot{x_{j1}} = \frac{A}{\tau_e} \cdot u_{TMS} + g \cdot LEd + C_1\sigma(C_2 v_{j3}) - \frac{2}{\tau_e}x_{j1} - \frac{1}{\tau_e^2}v_{j1} \tag{2}$$

2. Pyramidal intermediate second-order neurons

$$\dot{v}_{j2} = x_{j2} \tag{3}$$

$$\dot{x_{j2}} = \frac{B}{\tau_i}\left(C_4\sigma(C_3 v_{3j})\right) - \frac{2}{\tau_i}x_{j2} - \frac{1}{\tau_i^2}v_{j2} \tag{4}$$

3. Inhibitory neurons

$$\dot{v}_{j3} = x_{j3} \tag{5}$$

$$\dot{x_{j3}} = \frac{A}{\tau_e}\left(\sigma(v_{j1} - v_{j2})\right) - \frac{2}{\tau_e}x_{j3} - \frac{1}{\tau_e^2}v_{j3} \tag{6}$$

In the JR model, parameters A and B represent the maximum postsynaptic potential amplitudes of excitatory and inhibitory neuronal populations, respectively, while$\tau_e$and$\tau_i$denote the synaptic time constants for excitatory and inhibitory neuronal populations, respectively. C_1,C_2,C_3,and C_4 are key parameters describing the connection strengths between different neural populations. The parameter g represents the global gain factor, and u_TMS denotes the external input stimulus signal (such as TMS stimulation).

The JR model employs a sigmoid activation function to convert membrane potentials into neuronal firing rates, which are then transmitted as input signals to adjacent neuronal populations:

$$\sigma(x) = \frac{v_{max}}{1 + exp(r(v_0 - a))} \tag{7}$$

v_{max} represents the maximum firing frequency of neuronal populations, v_0 denotes the activation threshold of the sigmoid function, and r characterizes the response slope of the sigmoid function. Specifically, r_M,r_E, and r_I correspond to the firing rate parameters of Pyramidal Cells (PC), Excitatory Interneurons (EIN), and Inhibitory Interneurons (IIN), respectively

The Delayed Input mechanism is employed to simulate the time delay characteristics of neuronal activity signal transmission between different functional regions of the brain. This physiologically realistic modeling approach can more accurately reflect the biological processes of neural information transmission:

$$LEd = \sum_{j=1}^{N} w_{ij} \cdot E_j^{(t-\tau_{ij})} \tag{8}$$

w_{ij}represents the value of the structural connection matrix, $\tau_{ij} = {}^{d_{ij}}/_{v}$ delay is determined by the fiber bundle length d and the global axonal conduction velocity v. Finally, the channel-level EEG signal is calculated in the model. the difference between the excitatory and inhibitory interneuron activities of each cortical block is taken $r(t) = v_1(t) - v_2(t)$, the obtained source signal is multiplied by the leading matrix L, and then noise is added to obtain more realistic simulated data:

$$Y_{dy} = L * X + \epsilon \tag{9}$$

Masked Autoencoder

signals from partial observations. Its asymmetric encoder-decoder design maps masked signals to a latent space and reconstructs complete signals, enabling high-accuracy EEG reconstruction through deep learning.

This study focuses on learning resting-state EEG features from Alzheimer's Disease (AD) patients. Given dataset $D \in \{X_1, X_2, \cdots, X_L\}$, where each EEG sample $X_i \in \mathbb{R}^{C \times T}$ has C channels and T time points, we use partial masking to process signals. During fine-tuning, the model learns AD resting-state EEG characteristics, ensuring robust feature extraction when transitioning from masked (X) to real (X_real) signals.

In pretraining, the MAE reconstructs masked EEG data $X_i \in \mathbb{R}^{C_K \times T}$ from visible data $X_j \in \mathbb{R}^{C_j \times T}$, where C_K and C_j represent visible and masked channels. This initializes the feature extractor and recovers masked channel information. Using EEG data from both AD patients and Healthy Controls (HC), the model extracts shared features, improving generalization.

During fine-tuning, the pretrained model is optimized with AD resting-state EEG data. Specific masking strategies help capture AD-related patterns, enhancing feature extraction. This enables precise reconstruction and characterization of AD resting-state signals, supporting AD diagnosis and research.

The phased optimization approach ensures robust learning: pretraining captures general features across populations (AD and HC), while fine-tuning refines AD-specific features. This strategy enables efficient and accurate EEG signal processing, providing reliable tools for AD diagnosis and pathology studies.

Constraint loss

During the pretraining phase, the model learns shared features from both Alzheimer's Disease (AD) and Healthy Controls (HC) datasets, thereby acquiring the capability to reconstruct complete original signals from partially observed EEG signals (i.e., masked signals). The pretraining phase employs a reconstruction loss function to quantify the difference between the model's predictions and the original signals. For each EEG sample X_i, given its partial observation X_{mask} and the model's reconstructed signal $\hat{x}$, the reconstruction loss can be expressed as:

$$\mathcal{L}_{MAE} = \frac{1}{N}\sum_{i=1}^{N}\left\|X_{real}^{i} - \hat{X}^{i}\right\|^2 \tag{10}$$

where N represents the total number of samples in the dataset, X_{real}^{i} denotes the true EEG signal of the i-th sample, and $\hat{X}^{i}$ indicates the reconstructed EEG signal of the i-th sample by the model. During the fine-tuning phase, we exclusively utilize resting-state EEG datasets from AD patients for model optimization, enhancing the model's feature learning capability by masking partial EEG signals. Specifically, the pretrained model is further optimized using the AD dataset, and through the reconstruction and enhancement of AD-specific features, the model's ability to learn and characterize AD-related pathological patterns is significantly improved. Notably, during fine-tuning, we maintain the same reconstruction error calculation method as in the pretraining phase, ensuring the continuity and consistency of the model optimization process.

To extract dynamic feature patterns from EEG data and incorporate them as prior knowledge constraints in the optimization process of the Jansen-Rit (JR) dynamical model during the formal training phase, the loss function for formal training is defined as:

$$\mathcal{L} = \lambda_1 \cdot \mathcal{L}_{dy} + \lambda_2 \cdot \mathcal{L}_{pro} \tag{11}$$

The reconstruction loss L_dy of the JR dynamics model mainly includes the mean square error (MSE) between the simulated EEG data and the real EEG data and the complexity of the model (Momi et al., 2023):

$$\mathcal{L}_{dy} = \frac{1}{N_t}\sum_{t=1}^{N_t}\left(\frac{1}{N_{ch}}\sum_{i=1}^{N_{ch}}(y_i(t) - y_i'(t))^2\right) + ln\,\sigma + \frac{1}{\sigma^2}(\theta - \mu)^2 \tag{12}$$

Where N_t is the time point, N_{ch} is the number of electrode channels, and the model parameter θ is assumed to be a Gaussian distribution with a mean μ and a standard deviation σ.

$\mathcal{L}_{pro}$ is defined as the AD constraint loss function, whose primary objective is to ensure a high degree of similarity between the functional connectivity patterns of brain regions during TMS inter-stimulus intervals and AD resting-state functional connectivity. To achieve this constraint objective, we optimize model parameters by minimizing the functional connectivity differences between TMS inter-stimulus intervals and AD resting states, thereby effectively reducing the functional connectivity distance between them. However, it is important to note that $\mathcal{L}_{pro}$ is specifically designed to narrow the functional connectivity gap between healthy controls (HC) and AD patients, serving as a functional constraint during training. Despite this, the model's output remains focused on HC data, as $\mathcal{L}_{pro}$ is intentionally kept small to avoid overfitting to AD patterns while still guiding the model to learn relevant features. This approach ensures that the model retains its ability to generalize to HC data while incorporating AD-related insights for improved TMS response simulation.

$$\mathcal{L}_{pro} = \frac{1}{M}\sum_{i=1}^{M}\left\|C_{TMS-ISI}^{i} - C_{AD}^{i}\right\|^2 \tag{13}$$

Where $C_{TMS-ISI}^{i}$ is the brain region correlation matrix under TMS stimulation interval of the i-th sample, and C_{AD}^{i} is the AD resting state brain region correlation matrix of the i-th sample. The correlation can be calculated by the Pearson correlation coefficient:

$$C_{ij} = \frac{cov(X_i, X_j)}{\sigma_{X_i}\sigma_{X_j}} \tag{14}$$

Here, $cov(X_i, X_j)$ represents the covariance between the *i*-th and *j*-th brain regions, while σ_{X_i} and σ_{X_j} denote the standard deviations of the *i*-th and *j*-th brain regions, respectively. During this process, the parameters of the pre-trained model, which have already been optimized and fixed in the pre-training phase, are not updated further.

During the formal training phase, we utilize the functional connectivity matrices of Healthy Controls (HC) as input, with the corresponding output labeled as $Y_{Train} = Y_{HC}$.

Table 1: Performance comparison of models.

Fold/ACC	1	2	3	4	5	Mean
BEIT	54.20	49.64	74.30	71.05	62.09	62.25
MAE	**55.73**	**52.55**	**76.46**	**72.75**	**66.24**	**64.75**

Finally, in the model evaluation phase, the trained Jansen-Rit (JR) dynamical model is applied to the structural connectivity matrices of AD patients to directly predict the input data, with the output being the simulated neural response patterns of AD patients. This phased training strategy ensures that the model first learns the neural dynamic characteristics of healthy brains and then transfers this knowledge to simulate pathological states in AD patients.

$$Y_{test} = Y_{\mathrm{AD}} \tag{15}$$

Experiment

Datasets

Three public datasets were mainly used in this study:

1.The TMS-EEG open dataset provided by Rogasch et al. (2019) contains TMS-EEG recordings from 20 healthy participants aged 20-30 years (14 females). All data were collected with stimulation at the Primary Motor Cortex (M1) and have undergone preprocessing.

2.The OASIS-3 (Open Access Series of Imaging Studies 3) dataset is a publicly available, multimodal brain imaging dataset focusing on Alzheimer's Disease (AD) and normal aging processes. This study selected EEG data from 15 AD patients for analysis (LaMontagne et al., 2019).

3.The resting-state EEG dataset collected by the Second Department of Neurology at AHEPA University Hospital in Thessaloniki includes records from 88 participants. This study selected data from 36 AD patients (13 males) and 29 Healthy Controls (HC, 11 males) for analysis (Miltiadous et al., 2023).

Pre-trained AD Resting State Results

This study evaluated the accuracy of self-supervised EEG signal reconstruction using the Masked Autoencoder (MAE) framework, with BEIT serving as a comparative baseline. We compared their performance on resting-state EEG datasets from Alzheimer's Disease (AD) patients, using the Structural Similarity Index Measure (SSIM) to assess reconstruction quality. SSIM evaluates luminance, contrast, and structure, providing a comprehensive performance metric.

The experiment involved pretraining both MAE and BEIT on a mixed dataset of AD patients and Healthy Controls (HC), followed by fine-tuning on AD data. Pretraining enabled the models to learn common EEG features, with MAE achieving an SSIM of 0.53, outperforming BEIT (SSIM = 0.48). While demonstrating basic reconstruction capability, these results highlighted the need for fine-tuning to capture AD-specific patterns.

Fine-tuning on AD resting-state EEG data significantly improved MAE's ability to extract AD-related neural features. The SSIM increased to 0.65 ($p<0.05$), surpassing BEIT's fine-tuned performance (SSIM = 0.58). This improvement underscores the superiority of MAE in medical applications, enabling precise extraction of AD-specific neural patterns and supporting AD research and clinical diagnosis.

Dynamics simulation

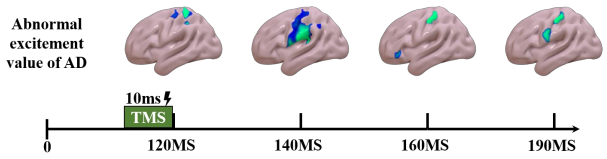

Figure 2: Simulated AD abnormal excitement value.

To evaluate neural response differences between Alzheimer's Disease (AD) patients and Healthy Controls (HC) under simulated Transcranial Magnetic Stimulation (TMS), we conducted paired-sample t-tests on neural activity data from 200 brain regions across 400 time points (12 AD vs. 12 HC). Results revealed significantly weaker neural responses in AD patients ($t = -9.99$, $p = 7.48 \times 10^{-7}$), supporting reduced cortical excitability in AD. After False Discovery Rate (FDR) correction, widespread neural response differences were observed between groups.

Building on these findings, we quantified cortical excitability differences using normalized neural activity: (AD-HC (mean))/HC (variance). Positive values indicate stronger neural activity in AD patients, reflecting enhanced excitability in specific regions or time windows. Figure 2 shows AD patients exhibited significantly increased excitability within a 70ms post-stimulation window, particularly in the sensorimotor cortex. Compared to controls, AD patients displayed prolonged localized neural activity (30-60ms) in stimulated regions, suggesting abnormal local circuit enhancement despite stronger motor cortex responses.

Our results align with research linking motor cortex hyperexcitability to AD patients and disease progression (Albers et al., 2015). Unlike traditional TMS methods, our TMS-EEG approach provides systematic cortical source-level analysis, revealing that motor cortex hyperexcitability may enhance local circuits while reducing overall network activity and connectivity.

These findings are supported by studies showing amyloid-β (Aβ) deposition in the motor cortex, similar to hippocampal damage (O'Leary et al., 2020). Aβ plaques disrupt synaptic

transmission, causing abnormal local circuits and network dysfunction (Koffie et al., 2009; Punzi et al., 2024), consistent with our observed localized activity enhancement. AD patients' distinct motor cortex activation patterns further suggest functional remodeling.

The pathological disinhibition observed, characterized by confined yet enhanced local responses, aligns with findings of non-target muscle activation in AD patients due to excitatory-inhibitory imbalance (Ferreri et al., 2011). This imbalance, driven by glutamatergic overactivation and weakened GABA inhibition (Sciaccaluga et al., 2021), explains the localized hyperexcitability in our results.

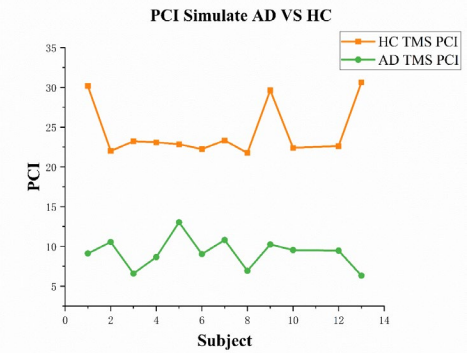

Figure 3: Perturbation complexity index (PCI) values to extracted from simulated TMS-EEG time series of AD and HC.

Furthermore, we compared the perturbation complexity index (PCI) between Alzheimer's disease (AD) patients and healthy controls (HC) to assess differences in neural responsiveness and consciousness levels under simulated conditions. This analysis complements our earlier findings on localized neural activity enhancement and cortical excitability differences, providing a broader perspective on how AD affects global brain dynamics. Figure 3 illustrates the simulated PCI values for both groups across various experimental conditions or individual subjects. The horizontal axis represents different subjects, while the vertical axis displays the corresponding PCI values. The blue line indicates PCI_sim_AD for AD patients, and the green line represents PCI_sim_HC for healthy controls.

As shown, the PCI values of the healthy control group are generally higher and exhibit greater fluctuations, reflecting the complex neural activity and higher level of consciousness in healthy brains when responding to external stimuli. This contrasts sharply with the patterns observed in AD patients, who show lower and less variable PCI values, likely due to neurodegenerative changes that reduce the brain's responsiveness to stimuli and impair consciousness levels (Parhizkar & Holtzman, 2022). These results align with our earlier observations of localized hyperexcitability and functional remodeling in AD patients, further underscoring the widespread impact of AD pathology on both local and global neural dynamics.

Conclusions

This study integrates deep learning with neural dynamics models to simulate and explore the dynamic responses of the nervous system in Alzheimer's disease (AD) patients under transcranial magnetic stimulation (TMS). By employing a masked autoencoder (MAE) to develop an AD-specific resting-state model and utilizing individualized functional connectivity matrices, the study enabled simulations and analysis of brain region responses to TMS. The results highlight regional heterogeneity in AD patients, showing increased excitability in stimulated specific regions. This localized hyperexcitability, accompanied by a global reduction in neural dynamics, is linked to AD pathological features, such as abnormal β-amyloid deposition and excitatory-inhibitory imbalance (Pichet Binette et al., 2024; Targa Dias Anastacio et al., 2022), offering new insights into the neural mechanisms of AD. AD patients exhibited enhanced cortical excitability in stimulated regions but lower perturbational complexity index (PCI) values, reflecting a dissociation between local hyperactivity and global network dysfunction. This pattern indicates impaired brain integration and responsiveness to stimuli, further supporting the notion of pathological disinhibition and excitatory-inhibitory imbalance in AD. These findings provide a novel perspective on AD neuropathology and underscore the potential of TMS as a tool for both understanding and treating AD.

Acknowledgments

This work was supported by the Chongqing Natural Science Fund Innovation and Development Joint Fund (Municipal Education Commission) project under Grant 2024NSCQ-LZX0058; the National Natural Science Foundation of China under Grant 62171074, W2411084; and the funding of Institute for Advanced Sciences of Chongqing University of Posts and Telecommunications under Grant E011A2022327.

References

Self, W. K., & Holtzman, D. M. (2023). Emerging diagnostics and therapeutics for Alzheimer disease. *Nature medicine*, 29, (pp.2187-2199).

Marucci, G., Buccioni, M., Dal Ben, D., Lambertucci, C., Volpini, R., & Amenta, F. (2021). Efficacy of acetylcholinesterase inhibitors in Alzheimer's disease. *Neuropharmacology*, 190, 108352.

Koch, G., Casula, E. P., Bonnì, S., Borghi, I., Assogna, M., Minei, M., ... & Martorana, A. (2022). Precuneus magnetic stimulation for Alzheimer's disease: a randomized, sham-controlled trial. *Brain*, 145, (pp.3776-3786).

Xiu, H., Liu, F., Hou, Y., Chen, X., & Tu, S. (2024). High-frequency repetitive transcranial magnetic stimulation (HF-rTMS) on global cognitive function of elderly in mild to moderate Alzheimer's disease: a systematic review and meta-analysis. *Neurological Sciences*, 45, (pp.13-25).

He, K., Chen, X., Xie, S., Li, Y., Dollár, P., & Girshick, R. (2022). Masked autoencoders are scalable vision learners.

In *Proceedings of the IEEE/CVF conference on computer vision and pattern recognition*, 1, (pp.16000-16009).

Brown, T., Mann, B., Ryder, N., Subbiah, M., Kaplan, J. D., Dhariwal, P., ... & Amodei, D. (2020). Language models are few-shot learners. *Advances in neural information processing systems*, 33, (pp.1877-1901).

Chen, F. L., Zhang, D. Z., Han, M. L., Chen, X. Y., Shi, J., Xu, S., & Xu, B. (2023). Vlp: A survey on vision-language pre-training. *Machine Intelligence Research*, 20, (pp.38-56).

Bricault, S., Dawson, M., Lee, J., Desai, M., Schwalm, M., Chung, K. S., ... & Jasanoff, A. (2024). Peripheral contributions to resting state brain dynamics. *Nature Communications*, *15*, 10820.

Griffiths, J. D., Bastiaens, S. P., & Kaboodvand, N. (2021). Whole-brain modelling: past, present, and future. In *Computational Modelling of the Brain: Modelling Approaches to Cells*, Circuits and Networks, 1, (pp. 313-355).

Elam, J. S., Glasser, M. F., Harms, M. P., Sotiropoulos, S. N., Andersson, J. L., Burgess, G. C., ... & Van Essen, D. C. (2021). The human connectome project: a retrospective. *NeuroImage*, 244, 118543.

Lavanga, M., Stumme, J., Yalcinkaya, B. H., Fousek, J., Jockwitz, C., Sheheitli, H., ... & Jirsa, V. (2023). The virtual aging brain: Causal inference supports interhemispheric dedifferentiation in healthy aging. *NeuroImage*, 283, 120403.

Mindlin, I., Herzog, R., Belloli, L., Manasova, D., Monge-Asensio, M., Vohryzek, J., ... & Sanz Perl, Y. (2024). Whole brain modelling for simulating pharmacological interventions on patients with disorders of consciousness. *Communications Biology*, 7, 1176.

López-González, A., Panda, R., Ponce-Alvarez, A., Zamora-López, G., Escrichs, A., Martial, C., ... & Deco, G. (2021). Loss of consciousness reduces the stability of brain hubs and the heterogeneity of brain dynamics. *Communications biology*, 4, 1037.

Sanchez-Rodriguez, L. M., Bezgin, G., Carbonell, F., Therriault, J., Fernandez-Arias, J., Servaes, S., ... & Iturria-Medina, Y. (2024). Personalized whole-brain neural mass models reveal combined Aβ and tau hyperexcitable influences in Alzheimer's disease. *Communications Biology*, *7*, 528.

Burt, J. B., Preller, K. H., Demirtas, M., Ji, J. L., Krystal, J. H., Vollenweider, F. X., ... & Murray, J. D. (2021). Transcriptomics-informed large-scale cortical model captures topography of pharmacological neuroimaging effects of LSD. *Elife*, 10, 69320.

Spiegler, A., Kiebel, S. J., Atay, F. M., & Knösche, T. R. (2010). Bifurcation analysis of neural mass models: Impact of extrinsic inputs and dendritic time constants. *NeuroImage*, 52, (pp.1041-1058).

Kaur, C., Singh, P., Bisht, A., Joshi, G., & Agrawal, S. (2022). Recent developments in spatio-temporal EEG source reconstruction techniques. *Wireless personal communications*, 122, (pp.1531-1558).

Momi, D., Wang, Z., & Griffiths, J. D. (2023). TMS-evoked responses are driven by recurrent large-scale network dynamics. *Elife*, 12, 83232

Biabani, M., Fornito, A., Mutanen, T. P., Morrow, J., & Rogasch, N. C. (2019). Characterizing and minimizing the contribution of sensory inputs to TMS-evoked potentials. *Brain stimulation*, 12, (pp.1537-1552).

LaMontagne, P. J., Benzinger, T. L., Morris, J. C., Keefe, S., Hornbeck, R., Xiong, C., ... & Marcus, D. (2019). OASIS-3: longitudinal neuroimaging, clinical, and cognitive dataset for normal aging and Alzheimer disease. *medrxiv*, 2019, 12.

Miltiadous, A., Tzimourta, K. D., Afrantou, T., Ioannidis, P., Grigoriadis, N., Tsalikakis, D. G., ... & Tzallas, A. T. (2023). A dataset of scalp EEG recordings of Alzheimer's disease, frontotemporal dementia and healthy subjects from routine EEG. *Data*, 8, 95.

Albers, M. W., Gilmore, G. C., Kaye, J., Murphy, C., Wingfield, A., Bennett, D. A., ... & Zhang, L. I. (2015). At the interface of sensory and motor dysfunctions and Alzheimer's disease. *Alzheimer's & Dementia*, 11, (pp.70-98).

O'Leary, T. P., Mantolino, H. M., Stover, K. R., & Brown, R. E. (2020). Age‐related deterioration of motor function in male and female 5xFAD mice from 3 to 16 months of age. Genes, *Brain and Behavior*, 19, 12538.

Koffie, R. M., Meyer-Luehmann, M., Hashimoto, T., Adams, K. W., Mielke, M. L., Garcia-Alloza, M., ... & Spires-Jones, T. L. (2009). Oligomeric amyloid β associates with postsynaptic densities and correlates with excitatory synapse loss near senile plaques. *Proceedings of the National Academy of Sciences*, 106, (pp.4012-4017).

Punzi, M., Sestieri, C., Picerni, E., Chiarelli, A. M., Padulo, C., Pizzi, A. D., ... & Sensi, S. L. (2024). Atrophy of hippocampal subfields and amygdala nuclei in subjects with mild cognitive impairment progressing to Alzheimer's disease. *Heliyon*, 10, 27429

Ferreri, F., Pasqualetti, P., Määttä, S., Ponzo, D., Guerra, A., Bressi, F., ... & Rossini, P. M. (2011). Motor cortex excitability in Alzheimer's disease: a transcranial magnetic stimulation follow-up study. *Neuroscience Letters*, 492, (pp.94-98).

Sciaccaluga, M., Megaro, A., Bellomo, G., Ruffolo, G., Romoli, M., Palma, E., & Costa, C. (2021). An unbalanced synaptic transmission: cause or consequence of the amyloid oligomers neurotoxicity?. *International Journal of Molecular Sciences*, 22, 5991.

Parhizkar, S., & Holtzman, D. M. (2022, January). APOE mediated neuroinflammation and neurodegeneration in Alzheimer's disease. In *Seminars in immunology*, 59, 101594

Targa Dias Anastacio, H., Matosin, N., & Ooi, L. (2022). Neuronal hyperexcitability in Alzheimer's disease: what are the drivers behind this aberrant phenotype?. *Translational psychiatry*, 12, 257.

Pichet Binette, A., Gaiteri, C., Wennström, M., Kumar, A., Hristovska, I., Spotorno, N., ... & Hansson, O. (2024). Proteomic changes in Alzheimer's disease associated with

progressive Aβ plaque and tau tangle pathologies. *Nature Neuroscience*, *27*, (pp.1880-1891).